

**Bimetallic-organic framework-derived Co-ZnO grown on carbon  
nanofibers as bifunctional electrocatalysis for rechargeable Zn-air batteries**

Xiaolan Wang<sup>a,b,c</sup>, Shaoshuai Xu<sup>a,b,c</sup>, Jie Bai<sup>a,b,c</sup>, Xingwei Sun<sup>\*a,b,c</sup> and Chunping Li<sup>\*a,b,c</sup>

<sup>a</sup>College of Chemical Engineering, Inner Mongolia University of Technology

<sup>b</sup>Inner Mongolia Key Laboratory of Green Chemical Engineering

<sup>c</sup>Key Laboratory of Industrial Catalysis at Universities of Inner Mongolia Autonomous  
Region

\*Corresponding authors: Xingwei Sun, Chunping Li

Tel: +86471 6575722.

Fax: +86471 6575722.

E-mail address: sxw@imut.edu.cn; hgcp\_li@126.com

## 1. Materials

Polyacrylonitrile (PAN,  $M_w = 80\ 000$ ), N, N-dimethylformamide (DMF, 98 %), potassium hydroxide (KOH,  $\geq 85\%$ ), methanol (99.5%), zinc acetate ( $Zn(OAc)_2$ , 99%), cobalt nitrate hexahydrate ( $Co(NO_3)_2 \cdot 6H_2O$ , 99%) and 2-methylimidazole (2-MI, 98%) were directly used without further purification. Carbon black and commercial Pt/C were obtained from Shanghai Hesen Electric Co. Ltd. Ruthenium oxide ( $RuO_2$ ) was chased from Aladdin. Deionized water was used for all the catalyst synthesis and electrochemical tests.

## 2. Physicochemical characterizations

The nanostructure of 2-MI/PAN, Co-Zn-ZIF/PAN, Co-ZIF/PAN, Co-Zn/CNFs and Co/CNFs were explored by scanning electron microscopy (SEM, Pro, Phenom, Netherlands). The lattice fringes and interfacial structures of nanomaterials were characterized by transmission electron microscopy (TEM, JEM-2100 JEOL, Japan). X-ray diffraction (XRD, Rigaku Ultima IV, Japan) analysis was conducted with a Cu  $K\alpha$  ( $\lambda = 0.15406\text{ nm}$ ) radiation source. The specific surface area and pore size distribution were determined using a Quanta chrome instrument (ASIQM-0001-3 instrument, USA). X ray photoelectron spectroscopy (XPS, Escalab 250 xi. Thermo Fisher Scientific USA) was carried out on Al  $K\alpha$  radiation source. The Raman spectroscopy (InVia Microscope Raman, Renishaw, England) was conducted on an argon laser source. Thermogravimetric analysis (TGA) was performed using STA-449F3 (NETZSCH Instruments, German). Temperature increases at  $5\text{ }^\circ\text{C}/\text{min}$  under nitrogen atmosphere.

## 3. Electrochemical measurements

All OER/ORR tests are performed using a three-electrode system.

OER: Catalyst ink was prepared by adding deionized water (100  $\mu\text{L}$ ), ethanol (98  $\mu\text{L}$ ) and Nafion solution (2  $\mu\text{L}$ ) to catalyst sample (1 mg). Drops were placed on carbon paper at a loading of  $1.5\text{ mg}/\text{cm}^2$ . Oxygen (99.9%) was filled into a four-mouth bottle containing 1.0 M KOH for 30 min before the test, followed by 50 cycles of cyclic voltammetry activation.

ORR: Catalyst ink was prepared in the same way as for OER. The catalyst ink (15  $\mu\text{L}$ ) was loaded onto a GC electrode ( $0.195\text{ mg}/\text{cm}^2$ ). Cyclic voltammetry (CV) studies were

performed in nitrogen- and oxygen-saturated 0.10 M KOH solution at a scan rate of 100 mV s<sup>-1</sup>.

The overpotential and electron transfer numbers were calculated using the following equations:

$$E_{RHE} = E_{SCE} + 0.0592 \text{ pH} + 0.241 \text{ V}$$

$$n = 4I_d / (I_d + I_r/N)$$

Which  $E_{RHE}$  is the potential vs. Reversible hydrogen electrode (RHE),  $E_{SCE}$  is the potential vs. calomel electrode, and pH is the pH value of electrode.

Double layer capacitors ( $C_{dl}$ ) were tested at different CV scan speeds of 20, 40, 60, 80, 100, and 120 mV s<sup>-1</sup>. The potentials were calculated by the formula:

$$E_{RHE} = E_{Hg/HgO} + 0.0592 \text{ pH} + 0.098 \text{ V}$$

Which  $E_{RHE}$  is the potential vs. Reversible hydrogen electrode (RHE),  $E_{Hg/HgO}$  is the potential vs. Hg/HgO electrode, and pH is the pH value of electrode.

The current density normalised by electrochemical active surface area was calculated using the following equation:

$$J_{ECSA} = \frac{I}{C_{dl}/C_s}$$

Where  $J_{ECSA}$  is the current density normalised by ECSA (mA cm<sup>-2</sup>);  $I$  is the current (mA);  $C_{dl}$  is the double layer capacitance,  $C_s$  is the specific capacitance for a 1 cm<sup>2</sup> flat surface, which is generally considered as 0.040 mF cm<sup>-2</sup> in alkaline solution.

Turnover frequency (TOF) values were calculated below:

$$\text{TOF} = j \times S / (z \times F \times n_{\text{metal}})$$

$S$  is the surface area coated by catalysts;  $j$  is the current density;  $z$  is the accepted or donated electrons for the generation of each H<sub>2</sub> or O<sub>2</sub> molecule (4 for OER/ORR process);  $F$  is the Faraday constant (96485.3 C mol<sup>-1</sup>);  $n_{\text{metal}}$  represents the amount of moles of all the active metal.

The zinc-air battery consisted of zinc foil, 6.0 M KOH and 0.2 M Zn(Ac)<sub>2</sub> electrolyte, Whatman TM glass microfiber spacer and nickel foam. The catalyst was formulated 1:1 with carbon black to form an ink (water (100 μL), ethanol (98 μL) and Nafion solution (2 μL))

drop on carbon paper (loaded with  $1.0 \text{ mg cm}^{-2}$ ). Pt/C+RuO<sub>2</sub> was loaded on carbon paper ( $1.0 \text{ mg cm}^{-2}$ ).

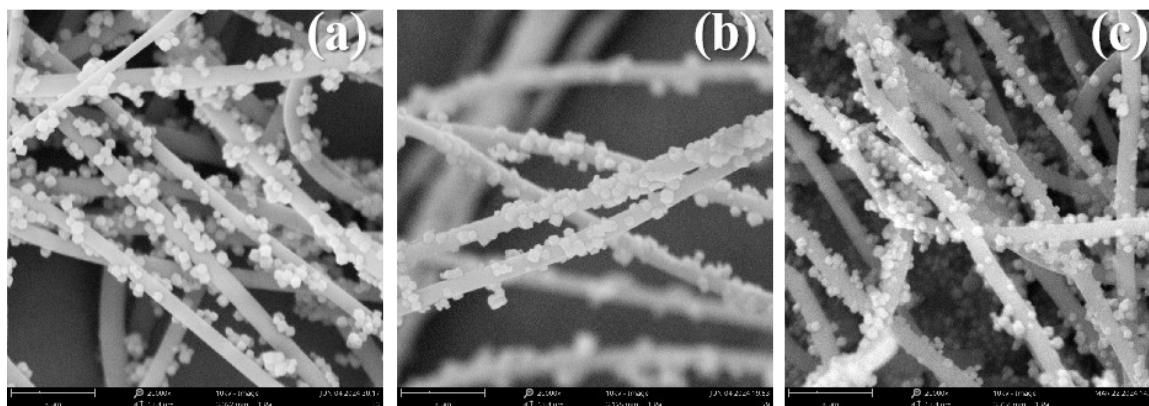


**Fig. S1** (a), (b), (c) and (d) SEM images of the Co-Zn-ZIF/PAN-4, Co-Zn-ZIF/PAN-1 and Co-ZIF/PAN, respectively.

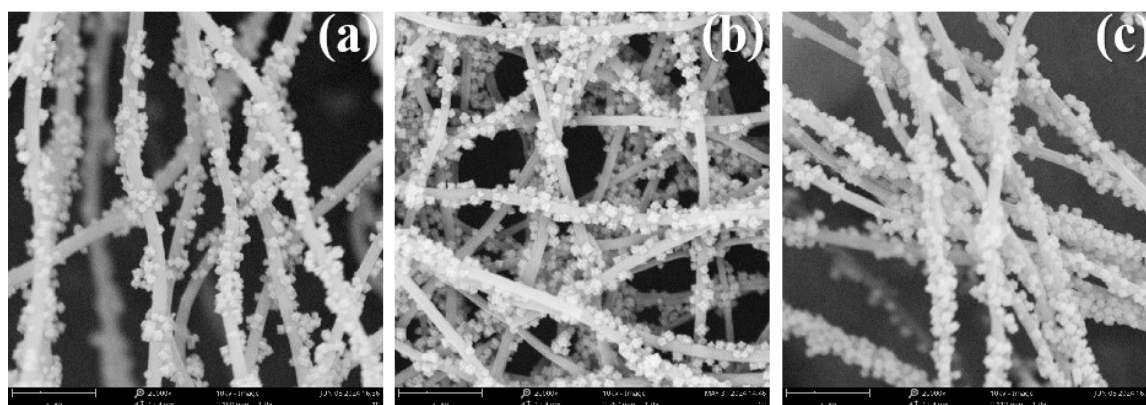


**Fig. S2** (a), (b), (c) and (d) SEM images of the Co-Zn/CNFs-4, Co-Zn/CNFs-1 and Co/CNFs, respectively.

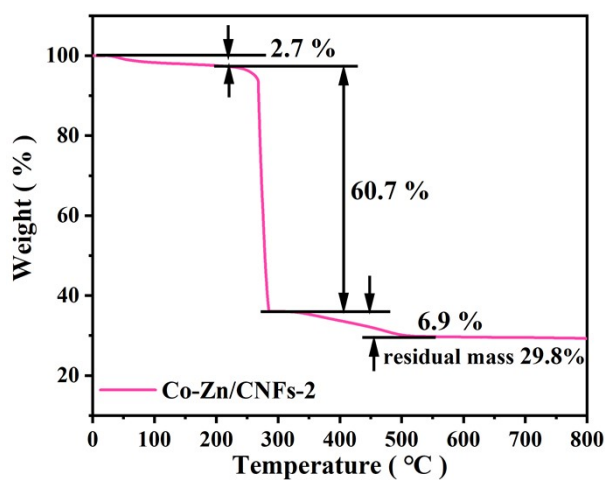


**Fig. S3** TGA curve of Co-Zn/CNFs-2.

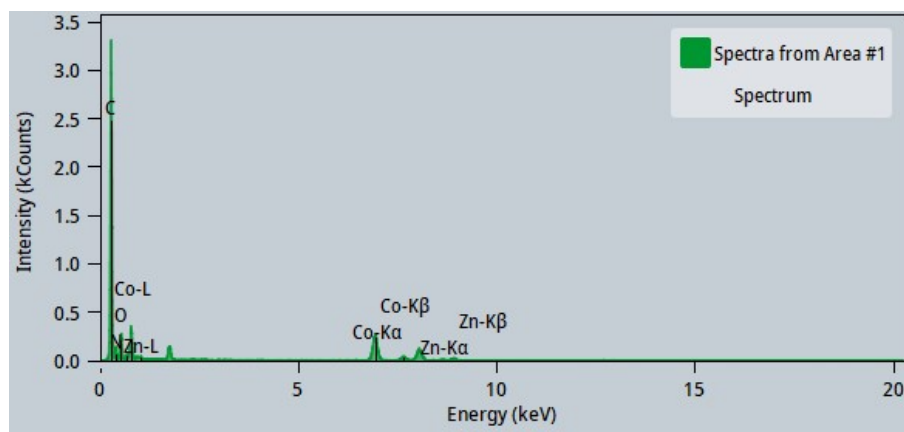


Fig. S4 EDX spectrum of Co-Zn/CNFs-2

Table S1 ICP-MS of Co-Zn/CNFs-2

Element	Co/wt%	Zn/wt%	Co/Zn atomic ratio
Atomic fraction (%)	18.41	1.10	31.2/1.7

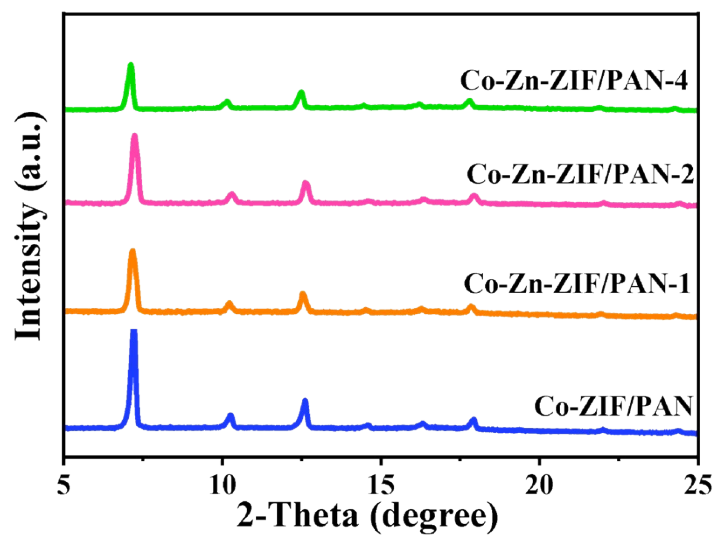


Fig. S5 XRD patterns of Co-Zn-ZIF/PAN-4, Co-Zn-ZIF/PAN-2, Co-Zn-ZIF/PAN-1 and Co-ZIF/PAN.

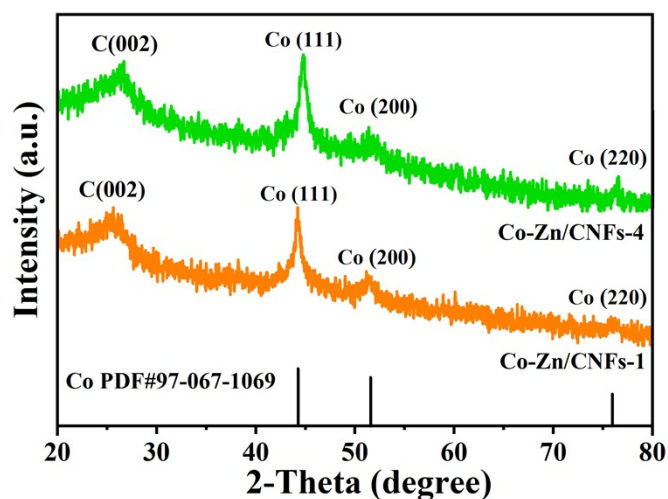


Fig. S6 XRD patterns of Co-Zn/CNFs-4 and Co-Zn/CNFs-1.

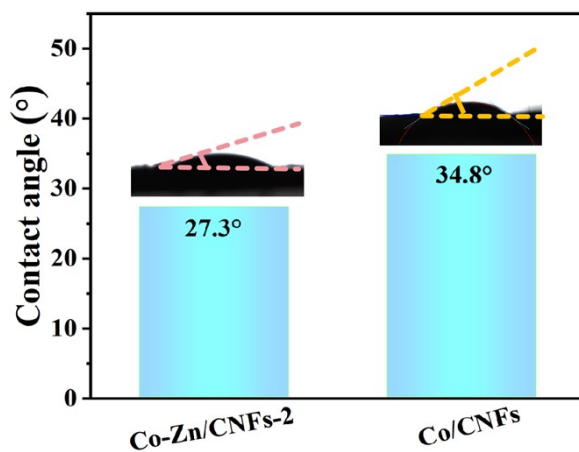


Fig. S7 Contact angles patterns of Co-Zn/CNFs-2 and Co/CNFs.

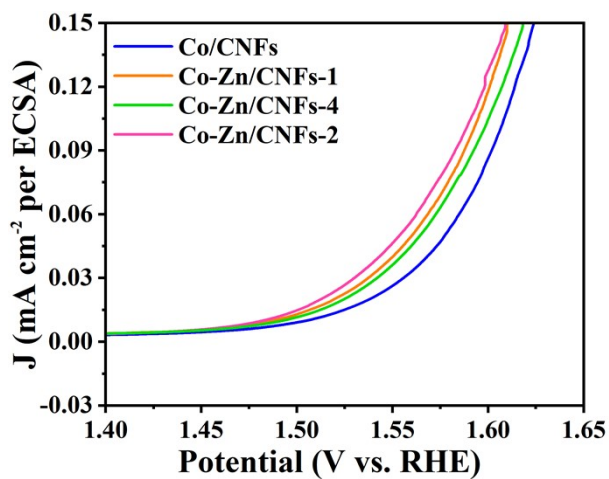
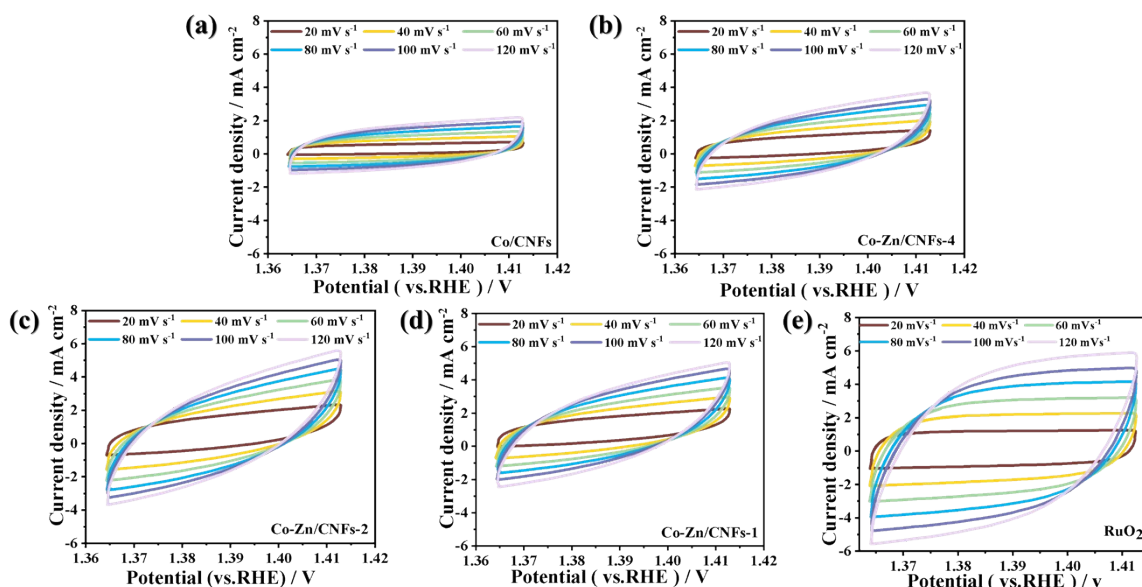
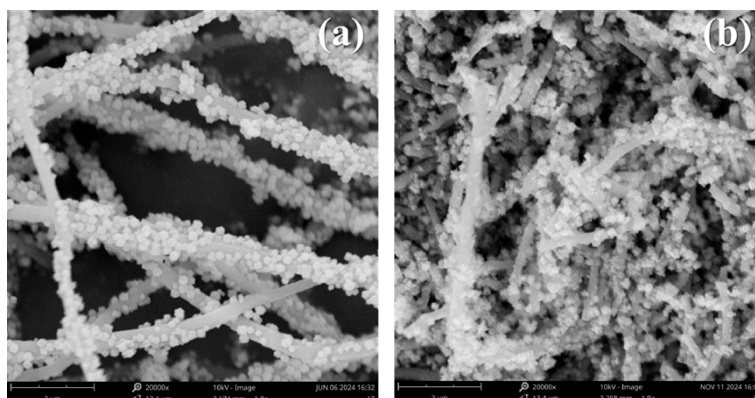


Fig.S8 ECSA-normalized LSV curves of different catalysts



**Fig. S9** The CV measurements in a non-faradic current region of (a) Co/CNFs, (b) Co-Zn/CNFs-4, (c) Co-Zn/CNFs-2, (d) Co-Zn/CNFs-1 and (e) RuO<sub>2</sub> at different scan rates of 20, 40, 60, 80, 100, and 120 mV s<sup>-1</sup>.



**Fig. S10** (a) and (b) SEM images of the Co-Zn/CNFs-2 before and after OER test.

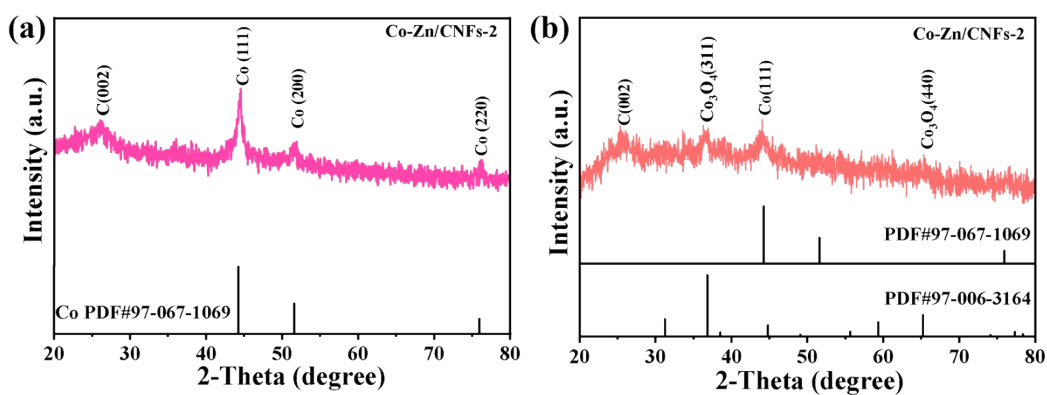


**Fig. S11** (a) and (b) XRD patterns of Co-Zn/CNFs-2 before and after OER test.

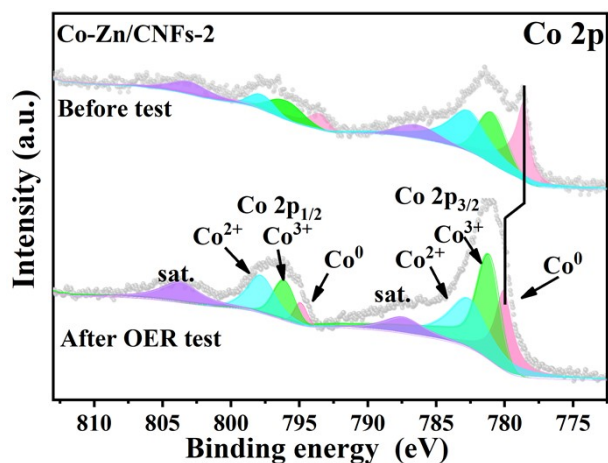


Fig. S12 XPS spectrum image of Co-Zn/CNFs-2 before and after OER test.

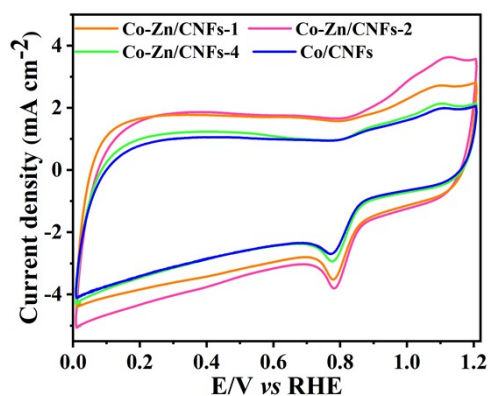


Fig. S13 CV curves of different catalysts in O<sub>2</sub>-saturated 0.1M KOH

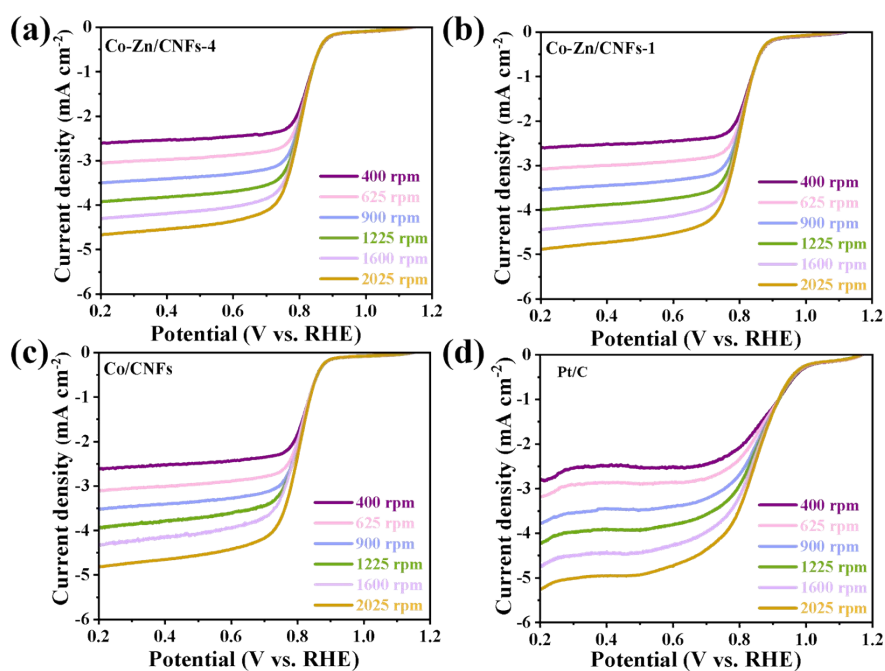
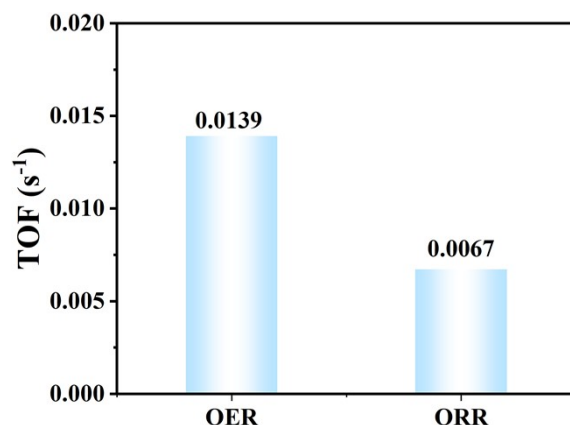
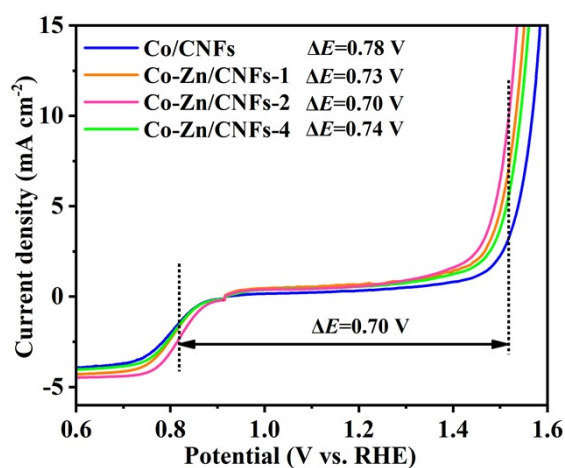


Fig. S14 (a), (b) and (c) LSV curves of Co-Zn/CNFs-4, Co-Zn/CNFs-1 and Co/CNFs samples at different rotation rates.



**Fig. S15** The TOF values for Co-Zn/CNFs-2 toward OER and ORR process.



**Fig. S16** Comparison of bifunctional activities of different samples

**Table S2** Comparison of the OER and ORR performance of different catalysts

Catalyst	$E_{j=10}$ (V vs. RHE)	$E_{1/2}$ (V vs. RHE)	$\Delta E$	Reference
Co-Zn/CNFs-2	1.52	0.816	0.70	This work
Co/Zn@NCF	1.69	0.84	0.85	Chemical Engineering Journal, 2023, 477: 147022
S-Co/CoNC	1.53	0.81	0.72	Materials Today Physics, 2023, 37: 101209
CNFs/CoZn- MOF@COF	1.57	0.82	0.75	Journal of Colloid and Interface Science, 2024, 666: 35
ZnCoFe-N-C	1.60	0.878	0.72	Small, 2023, 19(30): 2300612

CoNC-HCNFs	1.58	0.83	0.75	International Journal of Hydrogen Energy, 2023, 48(13): 5095
CoNi/Ti4O7@NS-CNFs	1.524	0.86	0.66	Journal of Colloid and Interface Science, 2023, 630: 763
ES-Co/Zn-CNZIFs	1.692	0.857	0.83	Journal of Energy Chemistry, 2023, 83:138
Co-N@PCNFs-0.2	1.66	0.87	0.79	ACS Sustainable Chemistry & Engineering, 2021, 9: 17068
NiFe-LDH/Co,N-CNF	1.542	0.790	0.75	Advanced Energy Materials, 2017, 7(21): 1700467
Co-N-CCNFMs	1.559	0.84	0.719	Energy Storage Materials, 2022, 47: 365
Co@Fe-CNFs-1000	—	0.81	—	Chinese Journal of Polymer Science, 2023, 41(12): 1889
ZIF-67@FeCo-NFs	1.62	0.89	0.73	Materials Today Energy, 2021, 20: 100682
CoZn/N-CNFs	—	0.814	—	Journal of Alloys and Compounds, 2023, 932: 167458
NiFe@C@Co CNFs	1.599	0.87	0.73	Small, 18(16): 2200578
Co/IMCCNFs	—	0.82	—	Nano-Micro Letters, 2019, 11: 1
Co-Fe-Zn@N-CNT/CNF	1.556	0.84	0.716	Inorganic chemistry, 2024, 63(9): 4373

**Table S3** Comparison of the peak power density of Zn-air batteries with various electrocatalysts

Catalyst	Peak power density (mW cm <sup>-2</sup> )	Reference
Co-Zn/CNFs-2	318.22	This work

---

ZnCo-NC-II	161.85	Applied Catalysis B: Environmental, 2022, 316: 121591.
CNFs/CoZn-MOF@COF	203.63	Journal of Colloid and Interface Science, 2024, 666: 35-46
ZnCoFe-N-C	137.8	Small, 2023, 19(30): 2300612
Co-N-C/CNF	159	Nano Research, 2023, 16(1): 545
CoZn/N-CNFs	223.8	Journal of Alloys and Compounds, 2023, 932: 167458
Co/Zn@NCF	202	Chemical Engineering Journal, 2023, 477: 147022
CoNi/Ti <sub>4</sub> O <sub>7</sub> @NS-CNFs	165.7	Journal of Colloid and Interface Science, 2023, 630: 763-771
Co-N@PCNFs-0.2	151	ACS Sustainable Chemistry &Engineering, 2021, 9, 17068-17077

---